Transport of dense colloids in porous media

Constantinos V. Chrysikopoulos[1], Vasileios E. Katzourakis[2] & Vasiliki I. Syngouna[2]

[1]School of Environmental Engineering, Technical University of Crete, 73100 Chania, Greece

[2]Environmental Engineering Laboratory, Department of Civil Engineering, University of Patras, 26500 Patras, Greece

P_4_2

Abstract

The role of gravitational force on dense-colloid transport in porous media was investigated. Transport experiments were performed with colloids in columns packed with glass beads placed in various orientations (horizontal, vertical, and diagonal). All experiments were conducted under electrostatically unfavorable conditions. The experimental data were fitted with a newly developed, analytical, one-dimensional, colloid transport model. The effect of gravity is incorporated in the mathematical model by combining the interstitial velocity (advection) with the settling velocity (gravity effect). The results revealed that flow direction influences colloid transport in porous media. The rate of particle deposition was shown to be greater for up-flow than for down-flow direction, suggesting that gravity was a significant driving force for colloid deposition. Furthermore, A three-dimensional numerical model was developed to investigate the simultaneous transport (cotransport) of dense colloids and viruses in homogeneous, water saturated, porous media with horizontal uniform flow.

Mathematical Developments

1-D Transport of Dense Colloids:

$$\frac{\partial C(t,x)}{\partial t}+\frac{\rho_b}{\theta}\frac{\partial C^*(t,x)}{\partial t}=D\frac{\partial^2 C(t,x)}{\partial x^2}-U_{tot}\frac{\partial C(t,x)}{\partial x}-\lambda C(t,x)-\lambda^*\frac{\rho_b}{\theta}C^*(t,x)$$

$$U_{tot}=U+U_{s(i)}$$

$$U_{s(i)}=-f_s\frac{(\rho_p-\rho_w)d_p^2}{18\mu_w}g_{(i)}$$

$$g_{(i)}=g_{(-z)}\sin\beta\ \mathbf{i}$$

$$\frac{\rho_b}{\theta}\frac{\partial C^*(t,x)}{\partial t}=k_c C(t,x)-k_r\frac{\rho_b}{\theta}C^*(t,x)-\lambda^*\frac{\rho_b}{\theta}C^*(t,x)$$

Initial & Boundary Conditions:

$$C(0,x)=0$$

$$-D\frac{\partial C(t,0)}{\partial x}+U_{tot}C(t,0)=\begin{cases}U_{tot}C_0 & 0<t\le t_p\\ 0 & t>t_p\end{cases}$$

$$\frac{\partial C(t,\infty)}{\partial x}=0$$

where

C_c Colloid particles suspended in the aqueous phase [M_c/L^3]

C_{c^*} Colloid particles attached onto the solid matrix [M_c/M_s]

C_v Viruses suspended in the aqueous phase [M_v/L^3]

C_{v^*} Viruses Directly attached onto the solid matrix [M_v/M_s]

C_{vc} Viruses attached onto suspended colloid particles [M_v/M_c]

$C_{v^*c^*}$ Viruses attached onto colloid particles already attached onto the solid matrix [M_v/M_c]

The various model parameters can be estimated by fitting the analytical solution to the experimental data with the nonlinear least squares regression package "Colloidfit."

The 3-D cotransport model assumes that the dense colloids exist in two different phases: suspended in the aqueous phase, and attached onto the solid matrix. The viruses are assumed to exist in four different phases: suspended in aqueous phase, attached onto the solid matrix, attached onto suspended colloids, and attached onto colloids already attached onto the solid matrix. The governing differential equations were solved numerically with appropriate finite difference schemes.

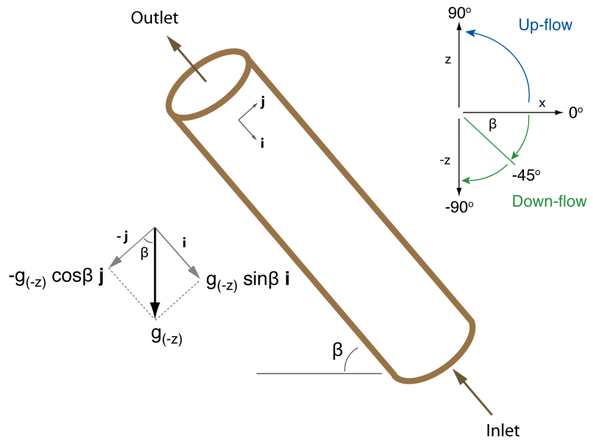

Figure 1. Schematic illustration of a packed column with up-flow velocity having orientation (-**i**) with respect to gravity.

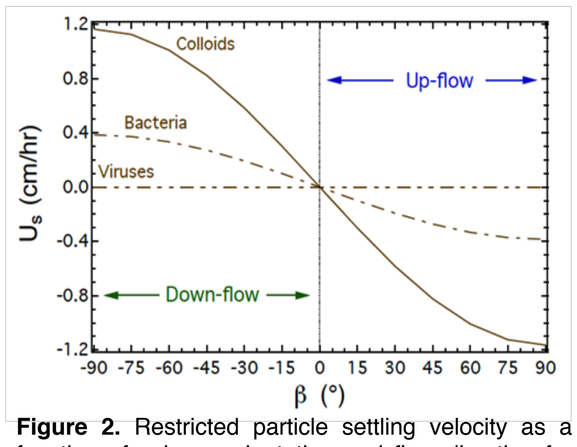

Figure 2. Restricted particle settling velocity as a function of column orientation and flow direction for colloids (clay: d_p=2 μm, ρ_p=2.65 g/cm³), bacteria (*P. putida*: d_p=2.2 μm, ρ_p=1.45 g/cm³), and viruses (bacteriophage MS2: d_p=25 nm, ρ_p=1.42 g/cm³). Here f_s=0.9.

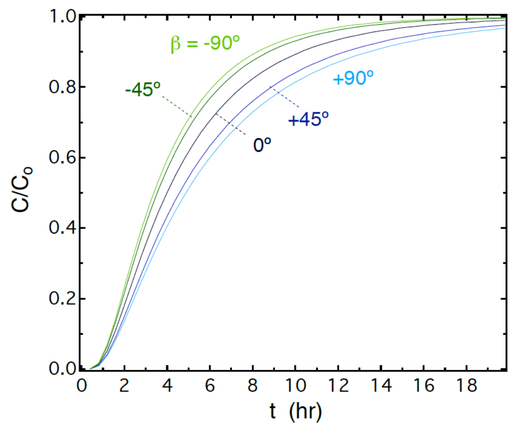

Figure 3. Simulations of normalized colloid break through curves for packed columns with various orientations and flow directions under continuous inlet boundary conditions.

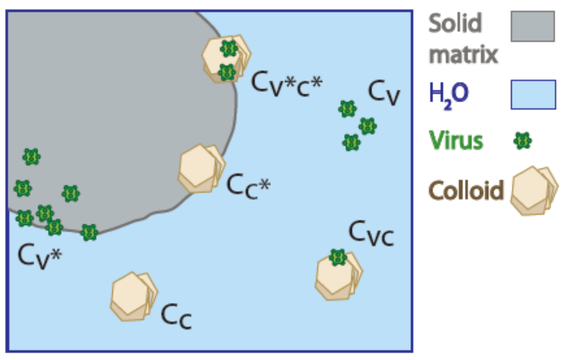

Figure 4. Schematic illustration of the various concentrations accounted for in the cotransport numerical model.

Experimental Approach

Colloids:

Kaolinite (KGa-1b) & Montmorillonite (STx-1b)

Column experiments:

Glass columns (2.5 cm diameter and 30 cm length), packing with d_p=2 mm glass beads, and Q=1.5 mL/min.

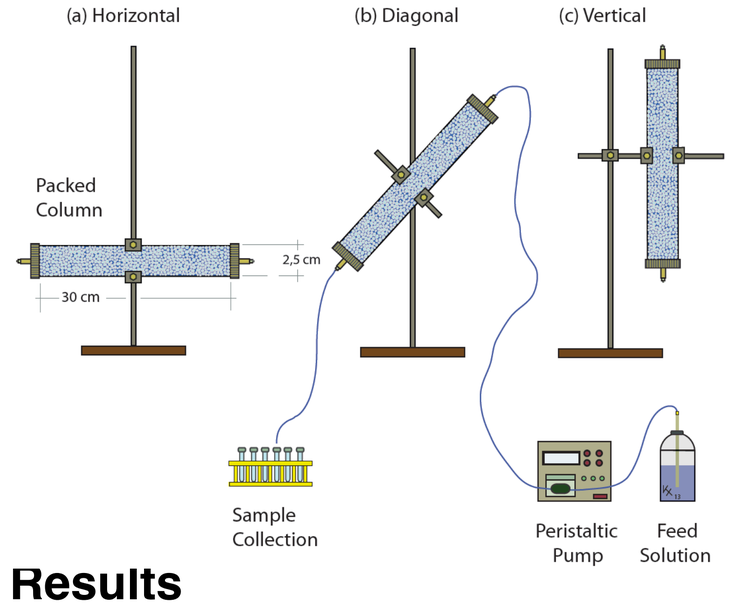

Figure 5. Experimental setup showing the various column arrangements: (a) horizontal, (b) diagonal, and (c) vertical.

Results

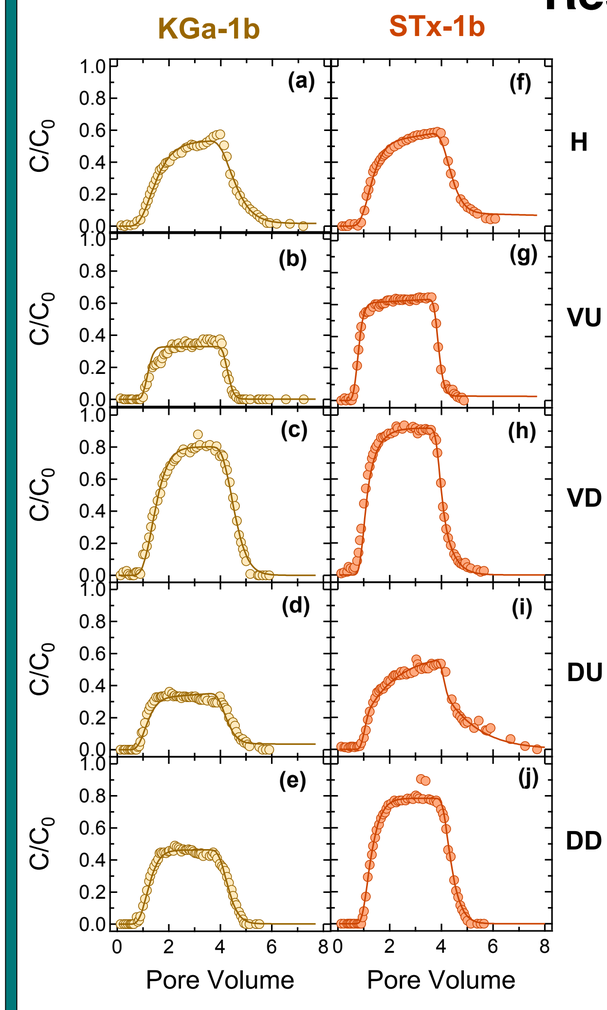

Figure 6. Experimental data (symbols) and fitted model simulations (curves) of (a-e) KGa-1b and (f-j) STx-1b breakthrough in columns packed with glass beads with (a,f) horizontal, (b,g) vertical up-flow, (c,h) vertical down-flow, (d,i) diagonal up-flow, and (e,j) diagonal down-flow directional flow conditions.

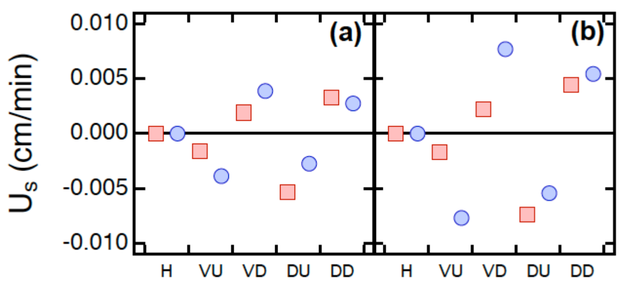

Figure 7. Comparison between theoretically estimated (circles), and fitted (squares) U_s values for: (a) KGa-1b, and (b) STx-1b. Here, $\rho_{KGa\text{-}1b}=\rho_{STx\text{-}1b}$=2.2 g/cm³, $U_{s(i)}<0$ for up-flow and $U_{s(i)}>0$ for down-flow experiments, H-horizontal, VU-vertical up-flow, VD-vertical down-flow, DU-diagonal up-flow, DD-diagonal down-flow.

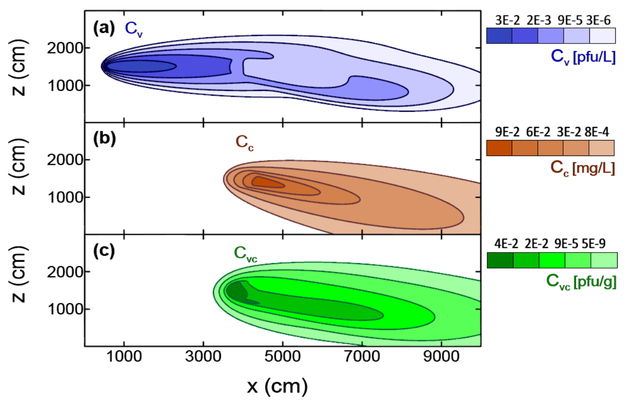

Figure 8. Concentration contour plots on the x-z plane for: (a) viruses, (b) colloids, and (c) virus-colloid particles during virus and colloid cotransport, accounting for gravitational effects. Here t=6900 hr, and y=15 m.

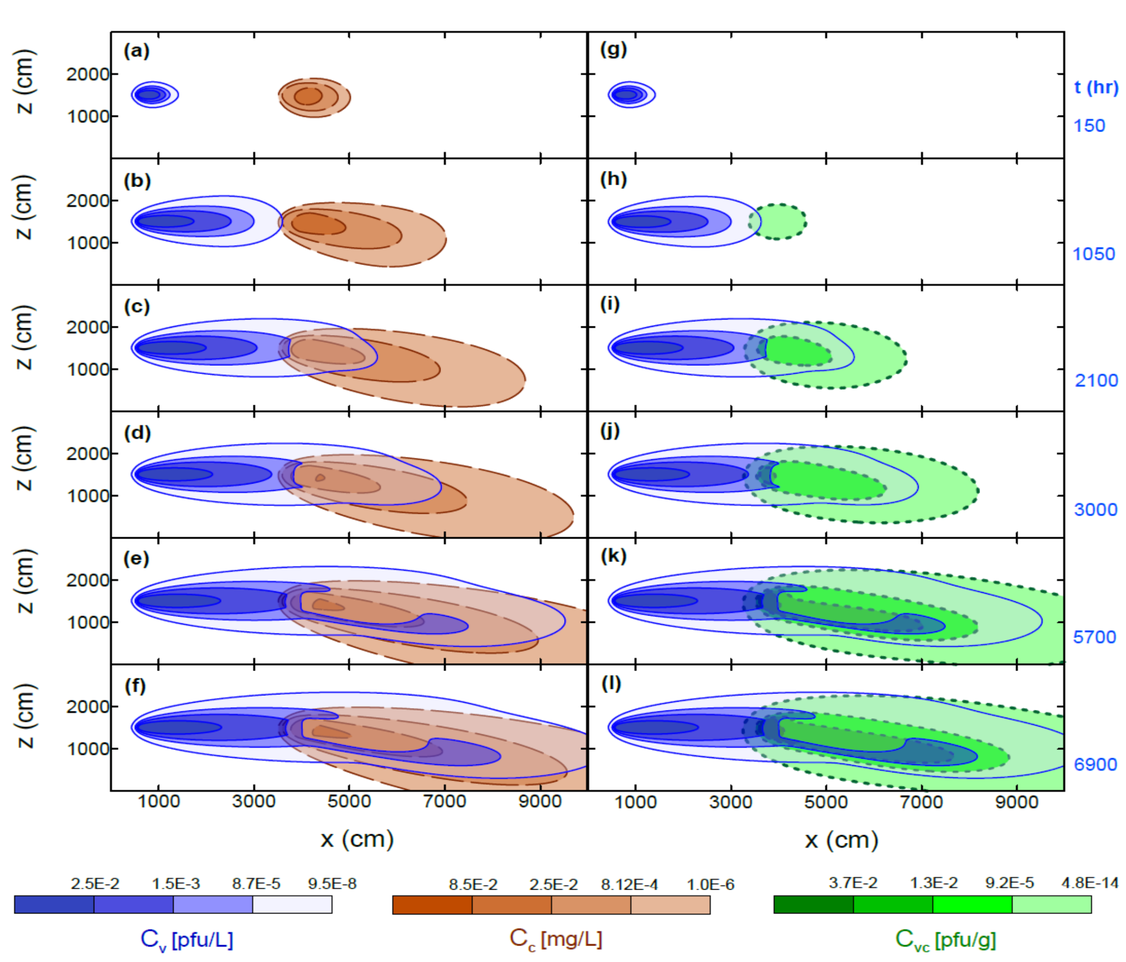

Figure 9. Concentration contour plots on the x-z plane for: (a) viruses, (b) colloids, and (c) virus-colloid particles during virus and colloid cotransport, accounting for gravitational effects. Here t=6900 hr, and y=15 m.

This research has been co-financed by the European Union (European Social Fund-ESF) and Greek National Funds through the Operational program "Education and Lifelong Learning" under the action Aristeia I (Code No. 1185). This work is a collaboration between members of the BioMet Network.